Defective osteogenesis of the stromal stem cells predisposes CD18-null mice to osteoporosis

Yasuo Miura*, Masako Miura†, Stan Gronthos‡, Matthew R. Allen§, Chunzhang Cao*, Thomas E. Uveges¶, Yanming Bi†, Driss Ehirchiou*, Angela Kortesidis‡, Songtao Shi†‖, and Li Zhang*‖

*Department of Physiology, University of Maryland School of Medicine, Rockville, MD 20855; †Craniofacial and Skeletal Diseases Branch, National Institute of Dental and Craniofacial Research, and ¶Bone and Extracellular Matrix Branch, National Institute of Child Health and Human Development, National Institutes of Health, Bethesda, MD 20892; ‡Mesenchymal Stem Cell Group, Division of Haematology, Institute of Medical and Veterinary Science, Adelaide 5000, South Australia, Australia; and §Department of Anatomy and Cell Biology, Indiana University School of Medicine, Indianapolis, IN 46202

Edited by Darwin J. Prockop, Tulane University, New Orleans, LA, and approved August 15, 2005 (received for review December 17, 2004)

Osteogenesis by the bone marrow stromal stem cells (BMSSCs) supports continuous bone formation and the homeostasis of the bone marrow microenvironment. The mechanism that controls the proliferation and differentiation of BMSSCs is not fully understood. Here, we report that CD18, a surface protein present primarily on hematopoietic cells, but not on differentiated mesenchymal cells, is expressed by the stromal stem cells and plays a critical role in the osteogenic process. Constitutive expression of CD18 on BMSSCs using a retroviral promoter significantly enhances bone formation *in vivo*, whereas genetic inactivation of CD18 in mice leads to defective osteogenesis due to decreased expression of the osteogenic master regulator Runx2/Cbfa1. The defective osteogenesis of the CD18-null BMSSCs can be restored by expressing full-length, but not cytoplasmic domain-truncated, CD18. Radiographic analyses with dual-energy x-ray absorptiometry and 3D microcomputed tomography show that mice lacking CD18 have decreased bone mineral density and exhibit certain features of osteoporosis. Altogether, this work demonstrates that CD18 functions critically in the osteogenesis of BMSSCs, and thus lack of CD18 expression in the leukocyte adhesion deficiency patients may predispose them to osteoporosis.

integrin | leukocyte adhesion deficiency | bone

Osteoporosis is characterized by excessive loss of bone and deterioration of bone tissue due to an overall imbalance between osteoblast-mediated bone formation and osteoclast-mediated bone resorption. Osteoblasts are derived from the bone marrow stromal stem cells (BMSSCs) (1) and play critical roles in the maintenance of bone mineral density (BMD) and in the formation of a bone marrow niche microenvironment that is essential for hematopoiesis (2, 3). When implanted s.c., the BMSSCs are capable of forming ectopic bone and bone marrow (4). Given their osteogenic capability, the *in vitro* expanded BMSSCs have been successfully used clinically to repair fractured bones (5). However, because of a lack of specific markers for stromal stem cells, isolation and *in vitro* expansion of highly purified BMSSCs in large quantity is still challenging.

Integrins are cell surface adhesion receptors and mediate cell–cell and cell–matrix interactions. Recent studies demonstrate essential roles of integrins, particularly the β_1, β_2, and β_3 subfamilies, in bone formation and remodeling. The β_1 integrins are expressed on chondrocytes and are important for their proliferation and the formation of the growth plate (6). The β_3 integrins are present on osteoclasts and are required for formation of the ruffled membrane borders on the bone surface. Thus, integrin β_3 is not essential for osteoclastogenesis but, rather, is critical to the bone-resorbing activity of the mature osteoclasts (7). Finally, the integrin $\alpha_L\beta_2$, one of the four β_2 (also termed CD18) integrins, is essential for *in vitro* osteoclastogenesis (8). However, its role in osteoclast maturation *in vivo* remains to be tested.

In human patients of the leukocyte adhesion deficiency type I, the majority of the mutations occur in the CD18 subunit, which abolishes surface expression of all four CD18 integrins ($\alpha_L\beta_2$, $\alpha_M\beta_2$, $\alpha_X\beta_2$, and $\alpha_D\beta_2$). Because of the prominent expression of CD18 on leukocytes, much attention in the past has been focused on the role of CD18 in leukocyte adhesion, migration, and immune responses. The impact of CD18 deficiency on bone formation has not been evaluated. In this work, we report that CD18 is expressed by BMSSCs, and CD18 deficiency abolishes osteogenesis, resulting in reduced BMD. Mice lacking CD18 display certain features of osteoporosis, including decreased BMD and increased trabecular bone space, suggesting that human leukocyte adhesion deficiency type I patients also could be predisposed to osteoporosis. Based on the differential expression pattern of CD18 on the differentiated mesenchymal cells vs. the BMSSCs, we speculated that CD18 could be a unique cell-sorting marker for the enrichment of human BMSSCs. We provided a proof of principle that combining CD18 with other stromal stem cell markers in cell sorting could significantly enhance the isolation of BMSSCs from human bone marrow aspirates. Altogether, our results demonstrate that CD18 plays a critical role in the osteogenesis of the BMSSCs, thus emphasizing the intimate relationship between the stromal stem cells and the hematopoietic stem cells (HSCs).

Methods

Mice. The CD18-null ($CD18^{-/-}$) mice and their sex-matched C57BL/6J littermates were obtained by breeding heterozygotes of the $CD18^{-/-}$ mice (9). The $CD18^{-/-}$ mice have been backcrossed by >10 generations into the C57BL/6J background. Animals were housed in a pathogen-free facility, and all procedures were performed with the approval of the Institutional Animal Care and Use Committee of the American Red Cross and the National Institute of Dental and Craniofacial Research.

BMSSC Culture and *in Vivo* Bone Formation Assay. Preparation and expansion of the BMSSCs was done based on methods described in refs. 4 and 10 (detailed methods are provided as *Supporting Materials and Methods*, which is published as supporting information on the PNAS web site). Briefly, mouse bone marrow mononuclear cells with the nonadherent cells removed were cultured on 10-cm culture dishes by using the irradiated guinea pig bone marrow as feeder cells. Human BMSSCs were prepared from human bone marrow aspirates of healthy adult volunteers, by using the above procedure but in the absence of the feeder cells. For *in vivo* bone formation, the expanded BMSSCs were

This paper was submitted directly (Track II) to the PNAS office.

Abbreviations: BMD, bone mineral density; BMSSC, bone marrow stromal stem cells; CFU-F, colony-forming unit fibroblast; HSC, hematopoietic stem cell; KO, knockout.

‖To whom correspondence may be addressed. E-mail: lizhang@som.umaryland.edu or sshi@mail.nih.gov.

www.pnas.org/cgi/doi/10.1073/pnas.0409397102

mixed with hydroxyapatite/tricalcium phosphate ceramic powder. The mixture was implanted s.c. into the dorsal surface of nude mice, and the implants were harvested at 7 weeks after implantation. Histological analysis and quantification of bone formation in the harvested implants were performed as described in ref. 11.

Enrichment of BMSSCs by FACS. Detailed procedures for enrichment of the BMSSC population by cell sorting are described in ref. 12 and also are provided in *Supporting Materials and Methods*. Briefly, bone marrow mononuclear cells were stained with mAb STRO-l (IgM), anti-IgM-biotin, streptavidin-microbeads, and finally streptavidin-FITC. The STRO-1^+ population were enriched by using a Mini MACS magnetic column (Miltenyi Biotec, Auburn, CA) and then stained sequentially with mAb 6.7 (against human CD18; IgG) and PE-conjugated anti-mouse IgG (both from Pharmingen) at 4°C. The STRO-1^{bright}/$CD18^+$ BMSSC population was enriched by dual-color cell sorting by using a FACSkfLus flow cytometer (Becton Dickinson). The sorted BMSSCs, either STRO-1^{bright}/$CD18^+$ or STRO-1^{bright}/$CD18^-$, were plated on the culture dishes and subjected to colony-forming unit fibroblast (CFU-F) assays based on the method described in ref. 13. Colonies were counted 12 days after cultivation.

***In Vitro* Differentiation Potentials of BMSSCs.** Osteogenic differentiation of BMSSCs was induced in the presence of 100 μM L-ascorbate-2-phosphate, 3 mM inorganic phosphate, and 10 nM dexamethasone. Mineral deposits were identified by Alizarin Red S staining after 3 weeks of cultivation (8). Adipogenesis was induced in α-MEM supplemented with 15% FBS, 100 μM L-ascorbate-2-phosphate, 0.5 mM isobutyl-methylxanthine, 0.5 μM hydrocortisone, 60 μM indomethacin, and 10 μg/ml recombinant human insulin. Oil Red O staining was used to identify lipid-laden fat cells after 2 weeks of cultivation, as described in ref. 9. Chondrogenic differentiation was assessed by Alcian blue staining of the cartilage matrix deposition in aggregate cultures treated with 100 μM L-ascorbate-2-phosphate, 2 mM sodium pyruvate, 1% insulin/transferring/selenous acid mixture (BD Biosciences), 100 nM dexamethasone, and 10 ng/ml TGF as described in ref. 10.

Analysis of Bone Phenotypes. Radiographs of mouse femurs were taken by Faxitron X-ray (Wheeling, IL). Quantitative analysis for BMD was based on dual x-ray absorptiometry by using a Piximus (GE Lunar, Madison, WI). Distal femoral metaphyses were analyzed by microcomputed tomography (μCT-20; Scanco Medical, Bassersdorf, Switzerland). To analyze the whole skeleton, 1-week-old mice were dissected to remove skin, muscle, and fat and kept in acetone to remove further fat for 3 days. They then were stained with 0.09% alizarin red S and 0.05% Alcian blue in a solution containing ethanol, glacial acetic acid, and water (67:5:28) for 48 h at 37°C. After staining, mice were transferred to 1% potassium hydroxide until the skeleton was clearly visible. Mice were preserved in 100% glycerol with gradual increase in concentration.

Osteoclast Activity. The tartrate-resistant acid phosphate staining was performed as described in ref. 14. Serum concentration of C-terminal telopeptides of type 1 collagen in mice was measured by using the Ratlap ELISA kit (Osteometer BioTech A/S, Herlev, Denmark).

Retroviral-Mediated CD18 Expression in BMSSCs. The CD18 cDNA was subcloned into the retroviral expression vector MGIN (15), and viral supernatants (6×10^6 cfu/ml) were prepared by using the packaging cell line GP+E-86 (16). CD18 expression on BMSSCs was achieved by viral infection (50–70% efficiency)

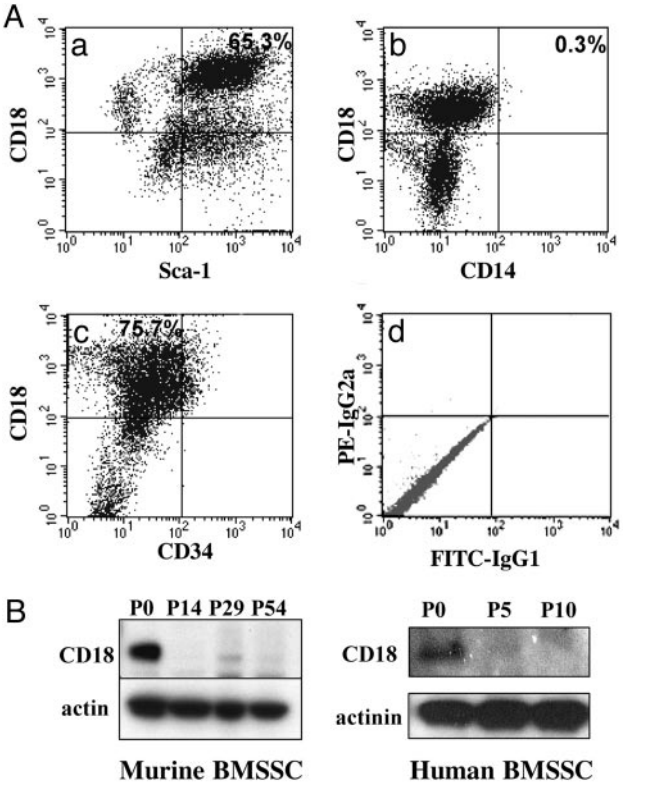

Fig. 1. CD18 is expressed by the BMSSCs. (*A*) Dual-color FACS analyses of the P0 murine BMSSCs, using mAbs specific for CD18, CD14, Sca-1, and CD34. (*d*) Isotype-matched IgGs were used as controls. (*b*) Lack of contaminating macrophages within P0 BMSSCs is demonstrated by the negative CD14 staining of $CD18^+$ BMSSCs. CD18 is coexpressed with Sca-1 (*a*) but not CD34 (*c*). The percentages of each population were shown in the quadrants. (*B*) Analysis of CD18 expression in murine and human BMSSCs by immunoblot, using a polyclonal Ab specific for CD18 cytoplasmic domain. CD18 expression was decreased in both murine and human BMSSCs upon consecutive cell passages. Equal protein loading was confirmed by reprobing with mAbs specific for β-actin or α-actinin. The data shown are representative of two independent experiments.

using our published methods (17) and was verified by FACS analysis using mAb C71/16 and by immunoblot using a polyclonal Ab against the cytoplasmic tail of CD18.

Analytical Methods. FACS analysis, immunoblot, cell adhesion assay, CFU-F assay, and BrdUrd labeling were conducted based on our published procedures (refs. 11 and 17; detailed methods also are provided in *Supporting Materials and Methods*).

Results

CD18 Is Expressed on BMSSCs and Can Be Used Efficiently as a Cell Surface Marker for Isolation of BMSSCs by Cell Sorting. CD18 is primarily expressed on cells of the hematopoietic origin (18). To examine whether CD18 is also expressed on BMSSCs, we generated murine BMSSCs from the wild-type (WT) mice under established culture conditions (4, 10) (a detailed description of the culture method can be found in *Supporting Materials and Methods*). Dual-color FACS analyses of the BMSSCs, which were derived directly from bone marrow without cell passage (i.e., passage 0), showed that a major cell population (≈65%) was double positive for CD18 and Sca-1 [a stromal stem cell marker (19)] (Fig. 1*Aa*). Expression of CD18 was not due to contaminating macrophages because the $CD18^+$ cells were negative for CD14, a commonly used macrophage marker (Fig. 1*Ab*). In addition, we found that the $CD18^+$ BMSSCs did not express

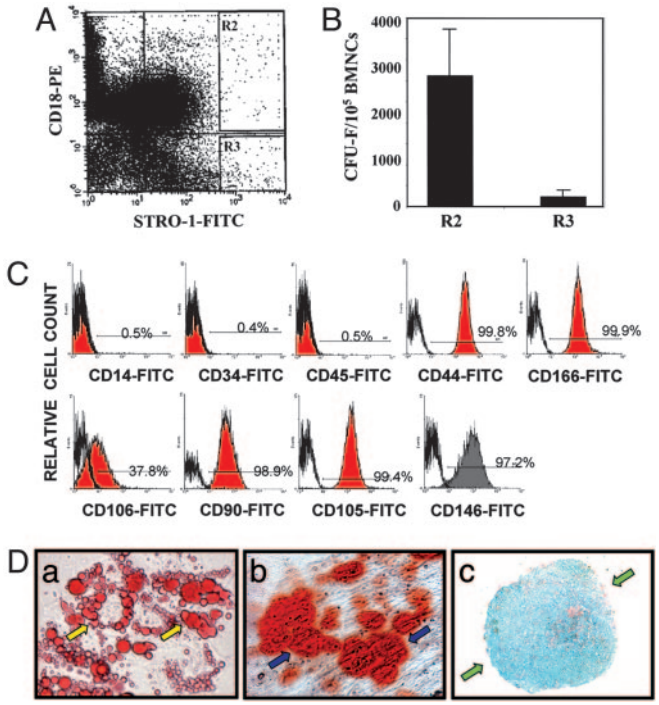

Fig. 2. Multipotent differentiation capability of the STRO-1^{bright}/CD18^{+} BMSSCs. (*A* and *B*) Enrichment of the STRO-1^{bright}/CD18^{+} BMSSC population by cell sorting. Fresh human bone marrow mononuclear cells were subjected to cell sorting using both STRO-1 and CD18 as specific markers. Two distinct cell populations (R2, STRO-1^{bright}/CD18^{+}; and R3, STRO-1^{bright}/CD18^{-}) were collected (*A*) and subjected to CFU-F assays (*B*). The STRO-1^{bright}/CD18^{+} cells formed much higher number of colonies than the STRO-1^{bright}/CD18^{-} cells. (*C*) Phenotypic characterization of the sorted human STRO-1^{bright}/CD18^{+} BMSSCs was performed by FACS analysis using different lineage-specific mAbs (filled in red). Their corresponding isotype-matched nonimmune IgGs were used as controls (bold line). The numbers given indicate the percentages of the positive cell population. Lack of macrophage contamination of the STRO-1^{bright}/CD18^{+} BMSSCs was demonstrated by the negative staining of either CD14 or CD45. (*D*) Differentiation potential of the STRO-1^{bright}/CD18^{+} BMSSCs. The sorted STRO-1^{bright}/CD18^{+} cells were cultured *in vitro* under adipogenic induction condition for 2 weeks (*a*), osteogenic induction condition for 3 weeks (*b*), and chondrogenic induction condition for 3 weeks (*c*). Oil Red O staining demonstrates the generation of lipid-laden adipocytes (yellow arrows) (*a*); Alizarin Red S staining shows mineral deposits (blue arrows) made by osteogenic cells (*b*); and Alcian blue staining of the cartilage matrix deposition (green arrows) demonstrates the chondrogenic differentiation in aggregate cultures (*c*). The data shown are representative of two independent experiments. (Magnification: *a* and *b*, ×400; *c*, ×64.)

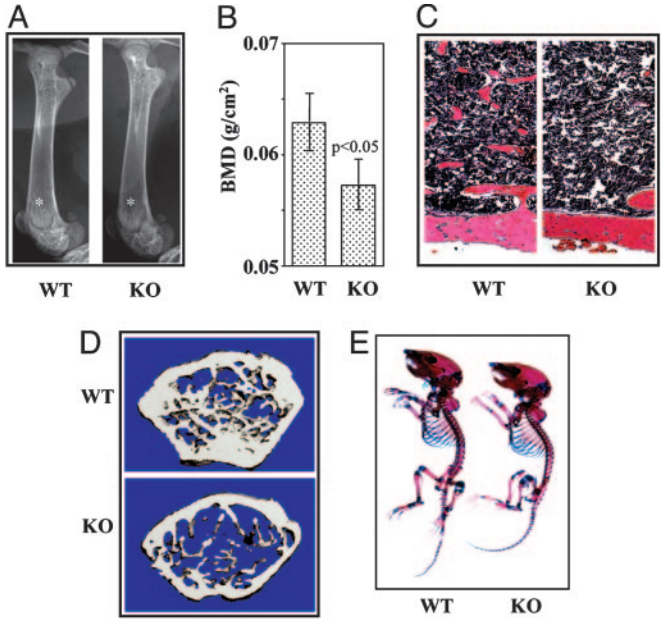

Fig. 3. Phenotypic comparisons between CD18$^{-/-}$ mice and their WT sex-matched littermates. (*A*) Faxitron analysis demonstrated a decreased bone density in the femurs of 5-week-old CD18$^{-/-}$ mice (KO, *Right*) as compared with their WT counterparts (*Left*). (*B*) Dual x-ray absorptiometry analysis of the femurs from 15-week-old mice showed a statistically significant difference in BMD between WT (left bar) and CD18$^{-/-}$ (right bar) mice ($P = 0.025$, $n = 4$). (*C*) Hematoxylin/eosin staining on the metaphysis area of the femurs showed diminished trabecular bone structure in CD18$^{-/-}$ (*Right*) mice as compared with WT mice (*Left*). (Magnification: ×400.) (*D*) Representative images of the distal femur metaphysis on microcomputed tomography analysis revealed decreased bone volume, trabecular bone number, trabecular bone thickness, and an increased trabecular bone space. (*E*) Alizarin red and Alcian blue double skeletal staining for bone (red) and cartilage (blue) of 1-week-old mice. KO, CD18$^{-/-}$.

CD34 (a HSC marker) (Fig. 1*Ac*). As further support, immunoblot analyses showed that both murine and human BMSSCs expressed CD18, and in both cases, the expression level decreased upon consecutive cell passages (Fig. 1*B*). Given the presence of CD18 on the BMSSCs, we tested the possibility of using CD18 as a selection marker for these stem cells, because identification of additional stem cell markers would be beneficial to stem cell purification and stem cell-based therapies (20). As proof of principle, we sorted BMSSCs from human bone marrow aspirates based on dual expression of CD18 (mAb 6.7) and the stromal stem cell marker, STRO-1 (12, 20–22) (Fig. 2*A*) and then determined the number of stromal stem/progenitor cells within the sorted cells by CFU-F assays (Fig. 2*B*). The results showed that dual-color FACS isolation of the bone marrow mononuclear cells coexpressing integrin CD18 and STRO-1 (Fig. 2*A*; R2, CD18^{+}STRO-1^{bright}) resulted in a 15-fold enhancement in the total number of BMSSC colonies (Fig. 2*B*) when compared with the CD18-negative population (R3, CD18^{-}STRO-1^{bright}). Phenotypical characterization of the CD18^{+}STRO-1^{bright} cells showed that they expressed CD44, CD166, CD106, CD90, CD105, and CD146, but not CD45 (a leukocyte marker), CD14 (a macrophage marker), or CD34 (Fig. 2*C*), which is consistent with the dual-color FACS results for murine BMSSCs (Fig. 1*A*). When cultured in specific differentiation-inducing conditions, the CD18^{+}STRO-1^{bright} cells were capable of differentiating into adipocytes (Fig. 2*Da*) osteoblasts (Fig. 2*Db*), and chondrocytes (Fig. 2*Dc*), thus confirming their differentiation potentials. Together, the above results demonstrate that integrin CD18 is expressed on BMSSCs and suggested that it could be used efficiently as a marker for cell sorting of the BMSSC population.

Mice Lacking CD18 Have Normal Skeletal Development but Exhibit Features of Osteoporosis. To determine whether CD18 played a role in the function of BMSSCs, we examined bone phenotypes of the CD18$^{-/-}$ [knockout (KO)] mice. Compared with their WT sex-matched littermates, genetic inactivation of CD18 led to a significant ($P < 0.05$) decrease in BMD of the femurs taken from both 5-week-old ($n = 3$) and 15-week-old ($n = 4$) mice, as assessed by Faxitron (Fig. 3*A*) and dual x-ray absorptiometry (Fig. 3*B*). The bone defects did not exacerbate with age between 5 and 15 weeks (data not shown), suggesting that the reduced BMD in the deficient animals was less likely due to chronic inflammation. Histological analysis of the femurs demonstrated that CD18$^{-/-}$ mice had decreased trabecular bones in the distal metaphysis (Fig. 3*C*), and microcomputed tomography analysis of the distal femur metaphysis indicated that bone volume, trabecular bone number, and trabecular bone thickness were

Table 1. Microcomputed tomography analysis of distal femoral metaphyses from 5-week-old mice

Indices	WT	KO	*P* value
BV/TV, %	17.8	8.52	0.0041
Tb.N, mm^{-1}	5.78	3.41	0.012
Tb.Th, μm^{-1}	31	25	0.022
Tb.Sp., μm^{-1}	151	348	0.035

Scanning regions were confined to secondary spongiosa and were ≈0.30 mm in thickness. Guided by the 2D images, a region of interest was manually drawn near the endocortical surface. Trabecular bone morphometric indices, including bone volume relative to tissue volume (BV/TV), trabecular number (Tb.N), trabecular thickness (Tb.Th), and trabecular separation (Tb.Sp), were assessed based on the reconstructed 3D images. WT, $n = 6$ mice; KO, $n = 7$ mice.

diminished, and trabecular bone space was increased in $CD18^{-/-}$ mice (Fig. 3*D* and Table 1). No significant defect in skeletal development was observed in $CD18^{-/-}$ mice as compared with their WT control mice littermates (1-week-old) (Fig. 3*E*).

Deficiency in CD18 Does Not Affect Overall Osteoclastic Activity. Proper BMD is maintained through a balance between osteoclast-mediated bone resorption and osteoblast-mediated bone formation (23), both of which require engagement of the integrin receptors. It is reported that chondrocyte-specific inactivation of integrin β_1 compromised bone development due to defective formation of the growth plate (6), and inactivation of integrin β_3 results in osteopetrosis due to defective bone absorbing activity of mature osteoclasts (7). Given that genetic deletion of $\alpha_L\beta_2$, whose expression is also defective in the $CD18^{-/-}$ mice, affects osteoclastogenesis (8), we anticipated that the osteoclastic activity in the $CD18^{-/-}$ mice should be decreased. To test this hypothesis, we carried out quantitative measurement of *in vivo* osteoclastic activity, based on the serum concentration of the C-terminal telopeptides of type 1 collagen, a commonly used marker for bone resorption (24). No significant difference between the deficient and WT mice was observed (Fig. 4*A*). To further evaluate the effect of CD18 deficiency on osteoclast formation, the total number of mature osteoclasts in the long bones of $CD18^{-/-}$ mice was quantified by tartrate-resistant acid phosphate staining (Fig. 4*B*; red), and no difference was found between the deficient and WT mice.

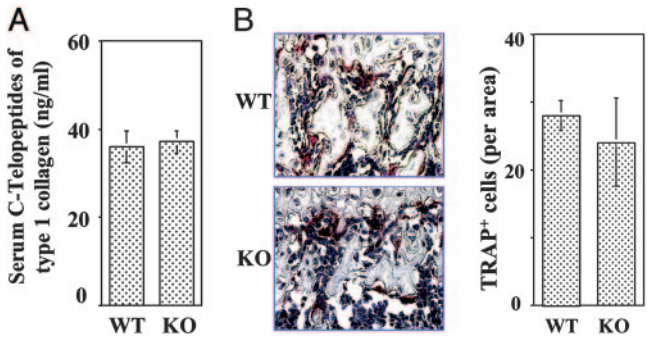

Fig. 4. $CD18^{-/-}$ mice exhibit normal osteoclastic activity. (*A*) *In vivo* osteoclastic activity was determined based on the serum concentration of C-terminal telopeptides of type 1 collagen. No significant difference in the total *in vivo* osteoclastic activity was observed between WT and the deficient mice ($P = 0.68$, $n = 3$ mice). (*B*) The number of mature osteoclasts in the femurs of the WT and $CD18^{-/-}$ mice was determined by tartrate-resistant acid phosphate staining. Similar numbers of osteoclasts were observed in WT and $CD18^{-/-}$ mice ($P = 0.13$, $n = 4$ mice). (Magnification: ×200.)

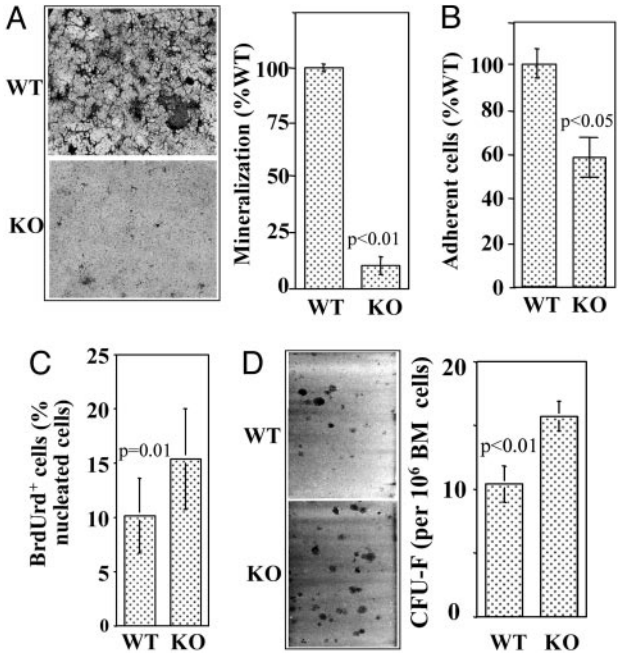

Fig. 5. CD18 deficiency compromises BMSSC differentiation but not proliferation. (*A*) *In vitro* mineralization induction of BMSSCs. Mineralization of the $CD18^{-/-}$ BMSSCs, determined by Alizarin red S staining (magnification: ×10), was significantly lower than that of WT cells ($P = 0.00003$, $n = 3$ mice). The total mineralized area by WT cells was assigned to 100%. (*B*) Cell adhesion. BMSSCs were allowed to adhere for 3 h at 37°C. After washing, the adherent cells were counted manually based on 10 randomly picked view fields and expressed as a percentage of WT cell adhesion. The $CD18^{-/-}$ BMSSCs adhered poorly compared with the WT cells ($P = 0.03$, $n = 4$). (*C*) Proliferation of BMSSCs was evaluated by BrdUrd incorporation, and the percentage of $BrdUrd^+$ cells was determined manually by counting 10 representative fields. $CD18^{-/-}$ BMSSCs proliferate better than the WT controls ($P = 0.01$, $n = 3$ mice). (*D*) CFU-F assay. The number of BMSSC colonies obtained from 10^6 bone marrow cells was significantly increased for the $CD18^{-/-}$ mice ($P = 0.0064$, $n = 6$ mice). (Magnification: ×10.)

CD18 Is Important for BMSSC Differentiation but Not for Proliferation. The above data suggest that osteoclast-mediated bone resorption is less likely responsible for the decreased bone formation in the $CD18^{-/-}$ mice. Therefore, we hypothesized that genetic inactivation of CD18 impaired osteogenic activity of the BMSSCs, leading to the observed decreased bone formation. To test this hypothesis, we performed *in vitro* mineralization induction assays on both WT and $CD18^{-/-}$ BMSSCs and found that mineralization by the $CD18^{-/-}$ BMSSCs was significantly lower ($P < 0.01$) than that by WT cells (Fig. 5*A*). In addition, $CD18^{-/-}$ BMSSCs adhered poorly to tissue culture dishes in comparison with their WT counterparts (Fig. 5*B*). Interestingly, the deficient BMSSCs proliferated better than the WT cells ($P = 0.01$) based on BrdUrd incorporation assays (Fig. 5*C*), and the bone marrow from $CD18^{-/-}$ mice contained higher numbers of single colony-derived BMSSCs (CFU-F) ($P < 0.01$) than that from WT mice (Fig. 5*D*).

Cbfa1 (Runx2/AML3/PEBP2αC) is a master regulatory gene in osteogenesis (25), and its biological effects are regulated by TGF-β through the Smad pathway (26, 27). We found that Cbfa1 expression in $CD18^{-/-}$ BMSSCs was decreased when compared with that of WT BMSSCs (Fig. 6*A Upper*). In addition, an increased response of Smad2 phosphorylation to TGF-β treatment was observed in $CD18^{-/-}$ BMSSCs (Fig. 6*A Lower*).

Expression of Full-Length CD18 in BMSSCs Promotes Osteogenesis. To further confirm the critical role of CD18 in BMSSCs-mediated

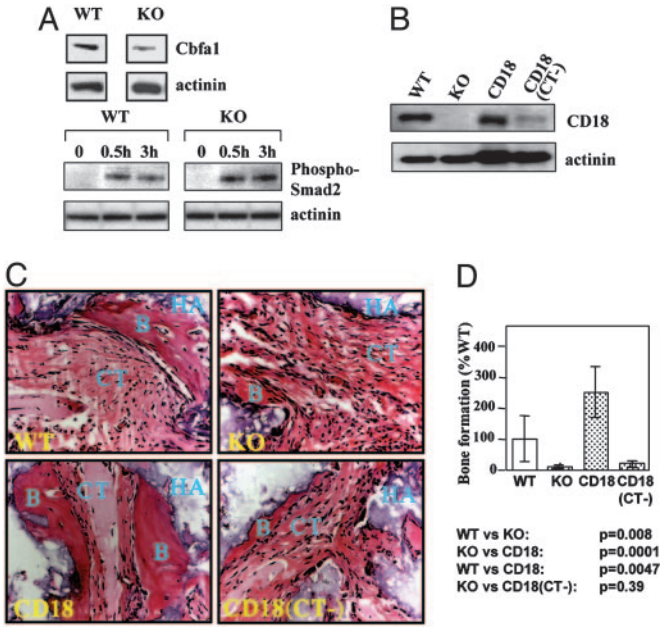

Fig. 6. Defective osteogenic capability of the CD18$^{-/-}$ BMSSCs. (*A*) Cbfa1 expression and Smad2 phosphorylation by immunoblot. Compared with WT cells, the CD18$^{-/-}$ BMSSCs exhibited decreased Cbfa1 expression (*Upper*) and enhanced response toward TGF-β stimulation, as indicated by Smad2 phosphorylation (*Lower*). Equal protein loading was verified by reprobing with an α-actinin-specific mAb. The data shown are representative of three independent experiments. (*B*) Retroviral mediated expression of recombinant CD18. The CD18$^{-/-}$ BMSSCs were infected with retroviral supernatants encoding either full-length CD18 or the cytoplasmic tail-truncated CD18 (CT−) for 6 days, and expression of recombinant CD18 was determined by immunoblot, using an anti-CD18 cytoplasmic tail Ab, which does not react well with CD18 (CT−). Noninfected WT and CD18$^{-/-}$ BMSSCs were included as controls, and protein loading was shown by reprobing for α-actinin. (*C*) Bone formation *in vivo*. WT, CD18$^{-/-}$, as well as the retroviral-infected CD18$^{-/-}$ BMSSCs with either CD18 or CD18 (CT−) were mixed with hydroxyapatite/tricalcium phosphate and then implanted s.c. in nude mice. The BMSSC-mediated bone formation was analyzed 7 weeks after implantation by hematoxylin/eosin staining. B, newly formed bone; HA, hydroxyapatite/tricalcium phosphate; CT, connective tissues. (Magnification: ×200.) (*D*) Restoration of the osteogenic capability of the CD18$^{-/-}$ BMSSCs. The amount of bone formation in *C* was quantified by using the software NIH IMAGE (http://rsb.info.nih.gov/nih-image) based on five representative areas and was expressed as a percentage of bone formation by WT BMSSCs. Bone formation by CD18$^{-/-}$ BMSSCs was significantly decreased compared with the WT BMSSCs ($P = 0.008$, $n = 4$ mice). The defective osteogenesis of CD18$^{-/-}$ BMSSCs was rescued by expression of CD18 ($P = 0.0001$, $n = 4$ mice) but not CD18 (CT−) ($P = 0.39$, $n = 4$ mice).

osteogenesis, and to exclude the possibility that CD18 contributes indirectly to osteogenesis through its function in hematopoetic cells, we conducted function–rescue experiments by expressing either full-length or cytoplasmic domain-truncated CD18, CD18 (CT−), in CD18$^{-/-}$ BMSSCs. Similar to WT BMSSCs, no macrophage contamination was detected in the P0 CD18$^{-/-}$ BMSSCs by FACS analysis (data not shown). To express recombinant CD18, the CD18$^{-/-}$ BMSSCs were infected with retroviruses carrying either full-length CD18 or mutant CD18 (CT−). Expression of recombinant CD18 on BMSSCs was confirmed 6 days after infection by immunoblot, using a polyclonal Ab against the cytoplasmic tail of CD18 (Fig. 6*B*). The osteogenic capability of WT BMSSCs, CD18$^{-/-}$ BMSSCs and the two different CD18-expressing CD18$^{-/-}$ BMSSCs was evaluated by using an *in vivo* model of ectopic bone formation (11). Consistent with the decreased osteogenic activity of the CD18$^{-/-}$ BMSSCs *in vitro* (Fig. 5*A*), we found that the CD18$^{-/-}$ BMSSCs failed to support bone formation *in vivo* (Fig. 6 *C* and *D*; WT vs. KO, $P = 0.016$), which was restored by the expression of full-length CD18 in the CD18$^{-/-}$ BMSSCs (KO vs. CD18, $P = 0.0001$). Surprisingly, the BMSSCs expressing CD18 constitutively by using the retroviral promoter exhibited significantly higher *in vivo* osteogenic activity (≈3-fold over WT BMSSCs; WT vs. CD18, $P = 0.0047$), indicating that prolonged expression of CD18 on BMSSCs enhances osteogenesis. In contrast, expression of a cytoplasmic domain-truncated CD18 failed to rescue the defective phenotype of bone formation [KO vs. CD18 (CT−), $P = 0.39$], suggesting that the cytoplasmic domain of CD18, which is required for integrin "outside-in" signaling, is required for the osteogenic differentiation of the BMSSCs.

Discussion

The stromal stem cells are potentially involved in the replenishment of a wide range of cell types through an adult life, including osteoblasts, chondrocytes, adipocytes, neural cells, and marrow stromal cells. Thus, BMSSCs represent an easily accessible and renewable source of stem cells for tissue engineering to repair damaged tissues (1). In addition, osteoblasts derived from BMSSCs are critical to the maintenance of the niche microenvironment for hematopoiesis (2, 3). However, because of the heterogeneity of BMSSCs and lack of specific surface markers for them, our understanding toward this type of stem cells is still limited. In this work, we identified a unique surface marker, CD18, for the BMSSCs and successfully used this previously undescribed stromal stem cell marker to enrich the BMSSCs population by cell sorting. Most importantly, we demonstrate that CD18 plays a critical role in osteogenesis of the BMSSCs, and mice lacking CD18 exhibit certain features of osteoporosis, including decreased BMD, reduced trabecular bone number, decreased trabecular bone thickness, and increased trabecular bone space.

It is surprising that CD18, a protein known to exist only on hematopoietic cell surface, is also expressed by the BMSSCs. Especially, we found that CD18 is highly expressed on the BMSSCs of the early passages after their purification from bone marrow. Given such a distinct pattern of expression, CD18 could be a useful surface marker for cell sorting to enrich the stromal stem cell population, because most of the other surface markers for stromal stem cells, including STRO-1, CD106/VCAM-1, CD146/MUC-18, HOP-26, CD49A/integrin β_1, and SB-10/CD166 (20, 22, 28), are expressed both on progenitor and on differentiated mesenchymal cells. As proof of principle, we isolated BMSSCs from human bone marrow aspirates by cell sorting using both CD18 and STRO-1, a cell marker commonly used for stromal stem cells (12). The number of stromal stem cells obtained in the CD18^{+}STRO-1^{bright} population was 15-fold higher than that of the CD18^{-}STRO-1^{bright} population, suggesting that only the CD18-expressing cells in the STRO-1^{bright} population are capable of self-renewal. Thus, this previously unidentified stromal stem marker should be helpful in the enrichment and *in vitro* expansion of the BMSSCs for therapeutic applications. Furthermore, because prolonged expression of CD18 on BMSSCs results in significantly enhancement of osteogenesis and bone formation (Fig. 6*D*), we anticipate that retroviral mediated expression of CD18 on BMSSCs could be beneficial to tissue engineering of bone and bone marrow.

In addition to CD18, another known HSC marker, Sca-1, also is expressed on stromal stem cells (19). Deficiency of Sca-1 leads to defects in HSC renewal (29) and mesenchymal stem cell renewal (30). As a result, Sca-1-deficient mice exhibit signs of osteoporosis, caused by both reduced bone formation and decreased bone resorption (30). Unlike Sca-1, we found that CD18 deficiency affected the differentiation, but not proliferation, of BMSSCs (Fig. 5). Whether CD18 deficiency also affects the differentiation and renewal of HSC is currently unclear and needs further investigation. It has been reported that CD18

deficiency causes severe leukocytosis (9), which may potentially lead to increased numbers of osteoclast precursor cells in the deficient mice. However, the defective expression of $\alpha_L\beta_2$ (one of the four CD18 integrins) in $CD18^{-/-}$ mice also decreases osteoclastogenesis (8). As a result, the overall osteoclastic activity in the $CD18^{-/-}$ mice remains unchanged (Fig. 4). Another interesting question that remains to be answered is whether the decreased differentiation of $CD18^{-/-}$ BMSSCs affects the niche microenvironment and therefore indirectly influences hematopoiesis. It is known that the $CD18^{-/-}$ HSCs can be easily mobilized into the blood circulation, due in part to the decreased HSC adhesion to bone marrow stroma (31). Our work suggests an additional possibility that CD18 deficiency in mice may affect the bone marrow stroma, thus diminishing the retention of HSCs within the bone marrow. Further studies will be required to test these hypotheses.

In conclusion, our work demonstrates that CD18 is a previously undescribed surface marker for both human and mouse BMSSCs. We provided a proof of principle that combining CD18 with other independent stromal stem cell markers (e.g., STRO-1, CD106/VCAM-1, and CD146/MUC-18) (20, 22) in cell sorting could significantly enrich the BMSSC population from unfractionated bone marrow aspirates, which could facilitate the use of purified and *in vitro* expanded BMSSCs for clinical application. Given the osteoporotic phenotype of the $CD18^{-/-}$ mice, our work suggests a strong possibility that patients with the severe form of leukocyte adhesion deficiency type I, including those with restored HSC functions by gene therapy, could be predisposed to bone defects and the development of osteoporosis. Thus, it would be necessary to include reconstitution of CD18 expression on both HSCs and BMSSCs for therapeutic treatments of the leukocyte adhesion deficiency type I patients in the future.

This work was supported in part by National Institutes of Health Grant NHLBI R01 HL61589-01 (to L.Z.), American Heart Association Grant 0240208N, and by an intramural program of the National Institute of Dental and Craniofacial Research, National Institutes of Health, Department of Health and Human Services. L.Z. is an Established Investigator of the American Heart Association.

1. Bianco, P. & Robey, P. G. (2001) *Nature* **414,** 118–121.
2. Zhang, J., Niu, C., Ye, L., Huang, H., He, X., Tong, W. G., Ross, J., Haug, J., Johnson, T., Feng, J. Q., *et al.* (2003) *Nature* **425,** 836–841.
3. Calvi, L. M., Adams, G. B., Weibrecht, K. W., Weber, J. M., Olson, D. P., Knight, M. C., Martin, R. P., Schipani, E., Divieti, P., Bringhurst, F. R., *et al.* (2003) *Nature* **425,** 841–846.
4. Krebsbach, P. H., Kuznetsov, S. A., Satomura, K., Emmons, R. V., Rowe, D. W. & Robey, P. G. (1997) *Transplantation* **63,** 1059–1069.
5. Quarto, R., Mastrogiacomo, M., Cancedda, R., Kutepov, S. M., Mukhachev, V., Lavroukov, A., Kon, E. & Marcacci, M. (2001) *N. Engl. J. Med.* **344,** 385–386.
6. Aszodi, A., Hunziker, E. B., Brakebusch, C. & Fassler, R. (2003) *Genes Dev.* **17,** 2465–2479.
7. McHugh, K. P., Hodivala-Dilke, K., Zheng, M. H., Namba, N., Lam, J., Novack, D., Feng, X., Ross, F. P., Hynes, R. O. & Teitelbaum, S. L. (2000) *J. Clin. Invest.* **105,** 433–440.
8. Tani-Ishii, N., Penninger, J. M., Matsumoto, G., Teranaka, T. & Umemoto, T. (2002) *J. Periodontal Res.* **37,** 184–191.
9. Scharffetter-Kochanek, K., Lu, H., Norman, K., van Nood, N., Munoz, F., Grabbe, S., McArthur, M., Lorenzo, I., Kaplan, S., Ley, K., *et al.* (1998) *J. Exp. Med.* **188,** 119–131.
10. Miura, M., Chen, X. D., Allen, M. R., Bi, Y., Gronthos, S., Seo, B. M., Lakhani, S., Flavell, R. A., Feng, X. H., Robey, P. G., *et al.* (2004) *J. Clin. Invest.* **114,** 1704–1713.
11. Shi, S., Gronthos, S., Chen, S., Reddi, A., Counter, C. M., Robey, P. G. & Wang, C. Y. (2002) *Nat. Biotechnol.* **20,** 587–591.
12. Gronthos, S., Graves, S. E., Ohta, S. & Simmons, P. J. (1994) *Blood* **84,** 4164–4173.
13. Kuznetsov, S. & Gehron, R. P. (1996) *Calcif. Tissue Int.* **59,** 265–270.
14. Baron, R., Neff, L., Tran, V. P., Nefussi, J. R. & Vignery, A. (1986) *Am. J. Pathol.* **122,** 363–378.
15. Cheng, L., Du, C., Murray, D., Tong, X., Zhang, Y. A., Chen, B. P. & Hawley, R. G. (1997) *Gene Ther.* **4,** 1013–1022.
16. Markowitz, D., Goff, S. & Bank, A. (1988) *J. Virol.* **62,** 1120–1124.
17. Xiong, Y. M., Chen, J. & Zhang, L. (2003) *J. Immunol.* **171,** 1042–1050.
18. Springer, T. A. (1990) *Nature* **346,** 425–434.
19. Van Vlasselaer, P., Falla, N., Snoeck, H. & Mathieu, E. (1994) *Blood* **84,** 753–763.
20. Gronthos, S., Zannettino, A. C., Hay, S. J., Shi, S., Graves, S. E., Kortesidis, A. & Simmons, P. J. (2003) *J. Cell Sci.* **116,** 1827–1835.
21. Simmons, P. J. & Torok-Storb, B. (1991) *Blood* **78,** 55–62.
22. Shi, S. & Gronthos, S. (2003) *J. Bone Miner. Res.* **18,** 696–704.
23. Bianco, P. & Gehron, R. P. (2000) *J. Clin. Invest.* **105,** 1663–1668.
24. Bonde, M., Qvist, P., Fledelius, C., Riis, B. J. & Christiansen, C. (1995) *J. Clin. Endocrinol. Metab.* **80,** 864–868.
25. Komori, T., Yagi, H., Nomura, S., Yamaguchi, A., Sasaki, K., Deguchi, K., Shimizu, Y., Bronson, R. T., Gao, Y. H., Inada, M., *et al.* (1997) *Cell* **89,** 755–764.
26. Miyazono, K., Maeda, S. & Imamura, T. (2004) *Oncogene* **23,** 4232–4237.
27. Alliston, T., Choy, L., Ducy, P., Karsenty, G. & Derynck, R. (2001) *EMBO J.* **20,** 2254–2272.
28. Stewart, K., Monk, P., Walsh, S., Jefferiss, C. M., Letchford, J. & Beresford, J. N. (2003) *Cell Tissue Res.* **313,** 281–290.
29. Ito, C. Y., Li, C. Y., Bernstein, A., Dick, J. E. & Stanford, W. L. (2003) *Blood* **101,** 517–523.
30. Bonyadi, M., Waldman, S. D., Liu, D., Aubin, J. E., Grynpas, M. D. & Stanford, W. L. (2003) *Proc. Natl. Acad. Sci. USA* **100,** 5840–5845.
31. Papayannopoulou, T., Priestley, G. V., Nakamoto, B., Zafiropoulos, V., Scott, L. M. & Harlan, J. M. (2001) *Blood* **97,** 1282–1288.